Iranian Journal of Astronomy and Astrophysics
Vol. 2, No. 2

Iranian Journal of Astronomy and Astrophysics

Proper integration time of polarization signals of internetwork regions using SUNRISE/IMaX data

Akram Gheidi Shahran · Taghi Mirtorabi
Physics Department, Alzahra University, Vanak, 1993891176, Tehran, Iran

Abstract. Distribution of magnetic fields in the quiet-Sun internetwork areas has been affected by weak polarization (in particular Stokes Q and U) signals. To improve the signal-to-noise ratio (SNR) of the weak polarization signals, several approaches, including temporal integrations, have been proposed in the literature. In this study, we aim to investigate a proper temporal-integration time with which an optimum SNR maintained physical properties is obtained. We use magnetographs of Zeeman sensitive Fe I 5250.2 Å line recorded by SUNRISE/IMaX to determine fraction of areas with significant polarization signals after temporal integrations with different durations. We examine several thresholds for the noise level. We also perform simple numerical simulations to explore the effect of size and lifetime of the magnetic features in obtaining the proper integration time. We find that the maximum fraction of pixels with real detectable linear polarization signals in the quiet-Sun internetwork is achieved with a maximum integration time about 8 minutes. Variation of polarization signals with integration time is strongly dependent on lifetime and size of magnetic patches. The temporal integration should be performed with great caution since in the presence of relatively long-lived magnetic features (such as network patches) SNR increases monotonically by increasing the integration time. This monotonic increase does not necessarily correspond to the internetwork areas where the linear magnetic features are relatively short-lived.

Keywords: Sun: photosphere – Sun: magnetic fields – techniques: polarimetric

1 Introduction

Recent investigations have shown that the quiet-Sun internetwork (IN), which occupies a large fraction of the solar surface may contain most of the unsigned magnetic flux at any given time [26], with much of the magnetic flux at the solar surface being in the form of horizontal fields [20, 19, 9]. The majority of individual magnetic features in these regions have been found to be small and relatively short-lived [18]. Therefore, only recent high spatial and temporal resolution observations (i.e., from Hinode and SUNRISE) have allowed studying the distribution of magnetic fields in the IN regions in more detail [21, 19, 24, 25, 2, 28, 7, 17]. It has been shown that only 25% of the IN areas may contain significant polarization signals (i.e., signals larger than 4.5 times the noise level) of Hinode/SP measurements with an integration time of 67.2s [23]. Hence, due to the small signal-to-noise ratio (SNR) in Stokes Q, U, and/or V, the magnetic field strength and orientation in many parts of the IN are still uncertain. These measurements have often been based on Stokes inversion techniques that may fail to return correct parameters (such as magnetic field strength or inclination angle) when the SNR in the linear polarization Stokes profiles is too low ([7, 2, 6]; cf. [17]).

Most controversial is the inclination of magnetic features in the IN. Thus, a pervasive horizontal field has been reported [20, 24, 19, 14, 23], or an isotropic distribution [2], or

even a predominantly vertical magnetic field [28]. Borrero et al. [7] have argued that contamination of Stokes Q, U, and V with photon noise leads to an overestimation of the horizontal component of the magnetic field. Because in the visible Q and U are generally weaker than Stokes V and hence are more likely to be swamped by noise. They performed several Monte Carlo simulations to retrieve through inversions the magnetic vector in pixels with predefined vertical field. They found that linear polarization signals that are not sufficiently above the noise caused the inversion code to return too horizontal fields. To achieve more reliable results, Borrero et al. [8] set up different selection criteria to single out pixels with high SNR, and found that due to the relative weakness of linear polarization signals compared to Stokes V, the selection based on only one of the Stokes parameters (i.e., where SNR of one of Stokes Q or U or V is larger than 4.5) may lead to a wrong result. They concluded that inversion codes retrieve the original (pre-defined) magnetic field when at least one of the linear components (Stokes Q or U) has an SNR of 4.5 or more. The latter criterion, however, restricts the number of invertible pixels to $5\% - 30\%$ of the entire area for the noise level of $\sigma = 1.0 \times 10^{-3}\ I_c$ and $\sigma = 2.8 \times 10^{-4}\ I_c$, respectively.

In their attempt to detect weak linear polarization signals, Lites et al. [19] temporally integrated the Hinode spectropolarimetric images over 67.2 s. Bellot et al. [4] extended the temporal integration of quiet-Sun Hinode/SP data to much longer integration times, and claimed to obtain the highest feasible SNR in the linear polarization signal. They reached an extremely low photon noise level of $7 \times 10^{-5}\ I_c$ after 25 min integration, which consequently led them to find that 69% of their quiet-Sun field-of-view (FOV) had at least SNR$\approx$ 4.5 in Stokes Q or U profiles. They also showed that even with an integration time of 10 min (with less image degradation compared to those with 25 min integration), about 60% of the internetwork had still a measurable linear polarization signal. In addition, they assumed that the linear polarization in the rest of the pixels with SNR$<$ 4.5 had to be real, since the Stokes Q and U in those pixels showed similar appearances in both Fe I 630 nm lines. From this, they concluded that "*the solar internetwork is pervaded by linear polarization signals*".

This is an interesting and to a certain extent also surprising result, since the Sun has significantly evolved within 25 minutes, or even 10 minutes. Within these times multiple generations of granules are born, evolve and die, moving magnetic features around. Many magnetic features in the IN also live less long than these integration times. In particular the more horizontal magnetic elements, detected in the linear polarization, are short-lived, at least as seen in photospheric observations [20, 9]. This can conceivably limit the integration time beyond which the reduction in the noise level in polarization signals is more than offset by the decrease in polarization signal due to motion-smearing and, in particular, the finite lifetimes of the magnetic features.

Here we extend the work of Bellot et al. [4] by integrating data recorded by IMaX on the first flight of Sunrise. These data complement those of Hinode /SP in that they were obtained by a filter instrument with a larger FOV and higher spatial resolution. The former property implies improved statistics, the latter a lower cut off in the size and hence possibly flux of magnetic features. In particular, we study the statistical behavior of noise and polarization signals from both observations and simple simulations. We investigate whether there is an integration time with which an optimum SNR can be achieved.

In Sect. 2 the data used in this study are described. Our analyses of the observational data and of the simulations are represented in Sect. 3. The last section is devoted to discussion and concluding remarks.

Table 1: Noise level (σ) of used dataset

σ_Q	σ_U	σ_V	σ_{LP}	σ_{CP}
8.3×10^{-4}	1.1×10^{-3}	1.0×10^{-3}	4.9×10^{-4}	5.2×10^{-4}

2 Data

We used a time series of 32 minutes duration acquired by IMaX magnetograph [22] on board the SUNRISE balloon-borne solar observatory [27, 3, 5, 10] on 9 June 2009. The FOV covers a 50×50 $arcsec^2$ of a quiet region near the center of the solar disk. Dataset consists of 58 consecutive frames of all four Stokes parameters of I, Q, U and V, with a cadence of 33 s and a pixel size of 0.055 arcsecs. Each polarization map was taken in five wavelength positions of ±40, ±80 and 227 mÅ from the center of line Fe I 5250.2 Å. The first four lie inside the absorption line while the last one located on a continuum point. The continuum images are used to estimate the noise level (i.e., the standard deviation of the continuum image).

The phase diversity reconstruction processing of data, increase the spatial resolution to 0.15 arcsecs that is two times larger than the resolution of non-reconstructed data, with the expense of increasing the noise by a factor of three [22]. Non-reconstructed (but flat fielded and corrected for instrumental effects) data with a lower noise are used in this work. To increase the SNR of polarization signals additionally, we average each of Stokes component over four wavelengths in the spectral line. It should be noted that total Q, U, V have a half of the noise of any individual wavelength summarised in Table 1. Also, we form the total linear polarization signal (LP) and circular polarization signal (CP) as follows:

$$LP = \frac{1}{4I_c} \sum_{i=1}^{4} \sqrt{Q_i^2 + U_i^2} \tag{1}$$

$$CP = \frac{1}{4I_c} \sum_{i=1}^{4} a_i V_i, \tag{2}$$

where i runs over the four wavelength positions, a is a vector equals to $[1, 1, -1, -1]$ [22], and I_c is the local continuum intensity taken from the fifth wavelength position. This definition of CP avoid any cancelation due to different signs in the blue and red wings of the absorption line.

3 Analysis

We expect that the SNR of circular and linear polarization signals should increase with increasing integration time of the data, if the magnetic patches in the quiet-Sun internetwork were to remain permanent and motionless, then we would expect an ideal increase in the SNR. For features with a finite lifetime, we expect there to be an 'ideal' integration time, i.e., one that leads to the largest increase in SNR. Integration times longer and shorter than this should lead to smaller enhancements in the SNR. For stationary magnetic features such

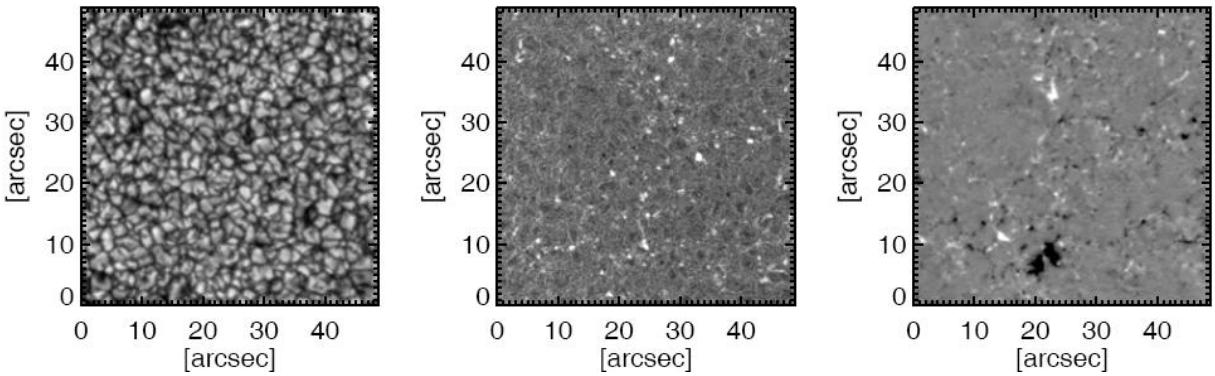

Figure 1: Continuum intensity map (left), linear polarization map (middle) and circular polarization map of SUNRISE/IMaX taken at quiet disk center on 9 June 2009.

an ideal integration time is expected to be comparable with the lifetimes of the magnetic features.

Horizontal magnetic features, located near the edges of granules, have been found to be smaller and shorter lived than more vertical magnetic elements that are concentrated in intergranular areas [19, 14, 9]. For the former a lifetime of 1-10 min is found, with a peak value at about 100 s [9, 14], while for the latter, a mean lifetime of 673 s [16] is found, assuming that vertical magnetic features are mostly associated with bright points. These limited lifetimes may be related to the lifetimes of the granules (of the order of 5-15 minutes; [1, 29, 13, 9]).

3.1 Temporal integration of SUNRISE/IMaX maps

In order to investigate the dependence of noise and the polarization signals on the integration time, we form the integrated images of IMaX as described in Sect. 2.

We also form the CP and the LP for each integrated map from their corresponding integrated images at each wavelength position, using Eqs. (2) and (1), respectively. Similarly, their noise levels are computed as the standard deviation of their integrated continuum positions. Figure 1 shows example maps of continuum intensity, linear polarization signals and circular polarization signals of IMaX data which we used in this work.

In Figure 2 variation of some parameters in terms of integration time are demonstrated. Plotted in Figure 2a, is the variation of rms contrast in the IMaX continuum intensity image. The values basically correspond to the granulation rms contrast (e.g. [12]). The contrast decreases through integration due to the proper motion, evolution and finite lifetime of the granules. It decreases from 8.2% for a single snapshot to 4.2% after integration time of 32 min.

It is important to note that all network patches have been excluded from the FOV prior to making these plots in the following, since we aim to investigate the polarization signals of internetwork areas only.

Reduction of the noise levels of Stokes Q, U, and V with the time integration is shown in Figure 2b (solid black line for Q, dotted blue line for U, and dashed red line for V). The noise levels are computed from the standard deviation of the continuum point of the corresponding Stokes images. After 30 minutes of integration, the noise level reduces to around $2 \times 10^{-4} - 3.5 \times 10^{-4}$.

Figures 2c and 2d are illustrated the fraction of the FOV covered by CP and LP signals larger than 4.5 times of noise level, versus integration time. From Figure 2c it can be seen that temporal integration amplifies the coverage of the FOV by significant CP signals for the first ≈ 5 minutes. For integration longer than this value, the CP coverage saturates at a relatively low level $\lesssim 14\%$ of the FOV. The surface coverage of pixels with detectable Stokes Q or U signals, i.e., these with SNR ≥ 4.5, do not increase monotonically with integration. An improving behavior is seen for surface coverage of Q or U signals up to an integration time of about 8 minutes then an overall gently decrease. Finally, it reaches to 2% of the FOV after 30 minutes integration time.

It is seen that the coverage of Q or U signals saturates at values an order of magnitude lower than that found by Bellot et al. [4]. Also, it should be noted that the increase in coverage of FOV by CP signals with temporal integration which not studied by them, is larger than that of Q or U coverage.

3.2 Temporal integration of synthesized maps

To test the results of the previous section from the observations and also investigate behavior of the variations of the polarization signals with integration time, we performed several simple numerical simulations.

3.2.1 Setup

We started by creating 60 blank frames of 500×500 $pixels^2$ in size. Each frame would represent a typical polarization map which could correspond to observational linear polarization image. At first a random noise with a normal distribution with a standard deviation of 4.9×10^{-4} (The same noise level as observational LP map) is added to all blank frames.

To simulate the linear polarization magnetic features, we created a set of magnetic patches each characterized by three quantities: size in pixels, lifetime in seconds (or number of consecutive frames they live) and amplitude. Danilovic et al. [9] found a rate of occurrence for the linear polarization magnetic patches equal to 7×10^{-4} s^{-1} $arcsec^{-2}$ for the IMaX images. To reproduce the occurrence rate in our synthetic frames, we added 1048 patches, in total, to the full set of 60 frames (i.e. about 17.5 patches in each frame, on average).

The distributions of the lifetime and size of the magnetic patches have also been taken from those obtained by Danilovic et al. [9] (Figures 2a and 2b in their paper). Exponentials with e-foldings of $\tau_T = 92$ s for the lifetime and $\tau_s = 0.24$ $arcsec^2$ for the size were fitted to the extended tail of their distributions. We use the correlations they obtained between size (S) and lifetime as well as between the maximum amplitude of linear polarization (LP_{max}) and the lifetime of linear patches (T), implying the following linear relationships:

$$S\,[pixel] = 0.66 \times T\,[second] + 11.2, \tag{3}$$

$$LP_{max}\,[\%] = 3.7 \times 10^{-4} \times T\,[second] + 0.15. \tag{4}$$

Also from Eq. 4, an exponential with e-folding of $\tau_{LP} = 7 \times 10^{-4}$ is fitted to the extended tail of the distribution of LP_{max}.

3.2.2 Assumptions and simplifications

We assumed a sudden birth and death for each patch with no growth rate, so that each magnetic patch displays a constant size and amplitude during its lifetime. Also, all the

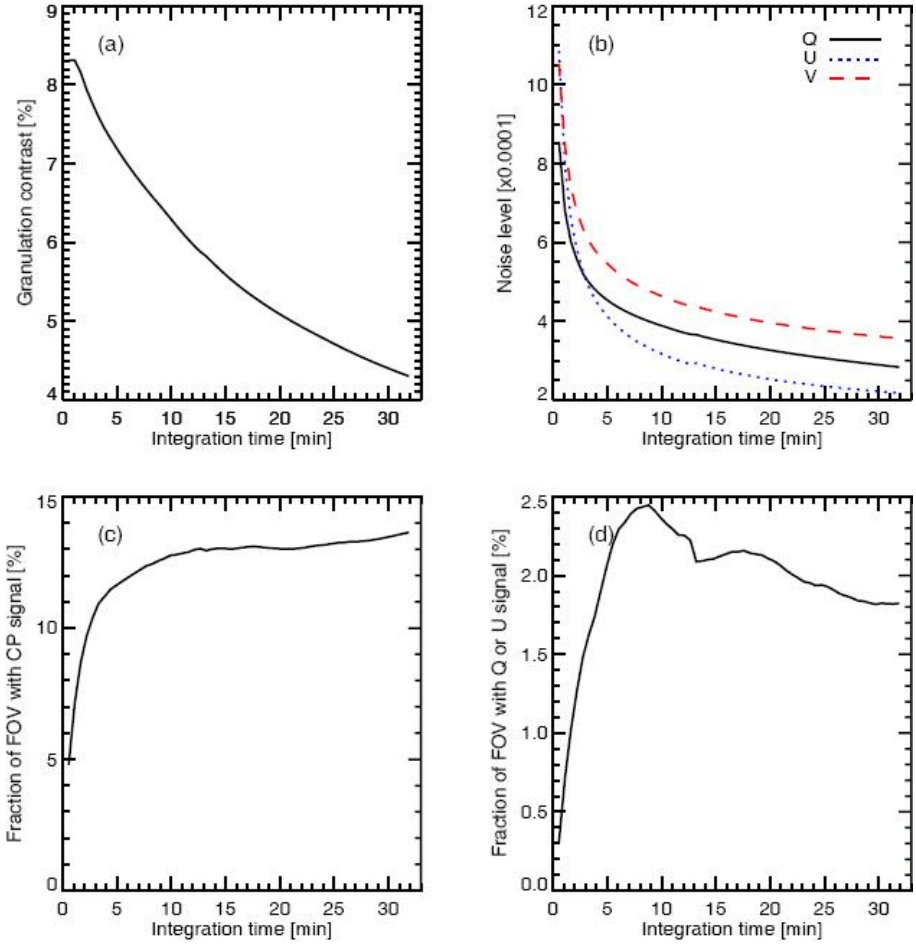

Figure 2: a) The rms continuum contrast versus integratin time. b) Noise levels of Stokes Q (solid black), U (dotted blue) and V (dashed red) as a function of integration time c) Fraction of field-of-view covered by circular polarization signals CP higher than 4.5 times of noise levels, versus integration time. d) Fraction of field-of-view covered by Q or U signals higher than 4.5 times of noise levels versus integration time.

pixels forming the patch surface, have the same amplitude of LP_{max}. This amplitude is determined according to the lifetime of the patch (Eq. 4)

In addition, the patches were assumed to be immobile. Thus, a patch appears in a random frame and stays alive and motionless in the next frames until its lifetime expires. The spatial motion of (horizontal and/or vertical) magnetic patches in the solar IN has been studied by several authors [9, 11, 15]. Horizontal motions reduce the statistical amplification of SNR by temporal integration. By assuming motionless magnetic patches, we determine an upper limit for SNR achievable by temporal integration of individual frames.

Furthermore, we combined these synthetic frames in the same way as we integrated the observed IMaX images in Sect 3.1 to explore the fraction al area covered by LP signals for different integration times.

In order to investigate the influence of individual quantities (i.e., lifetime, size, and LP

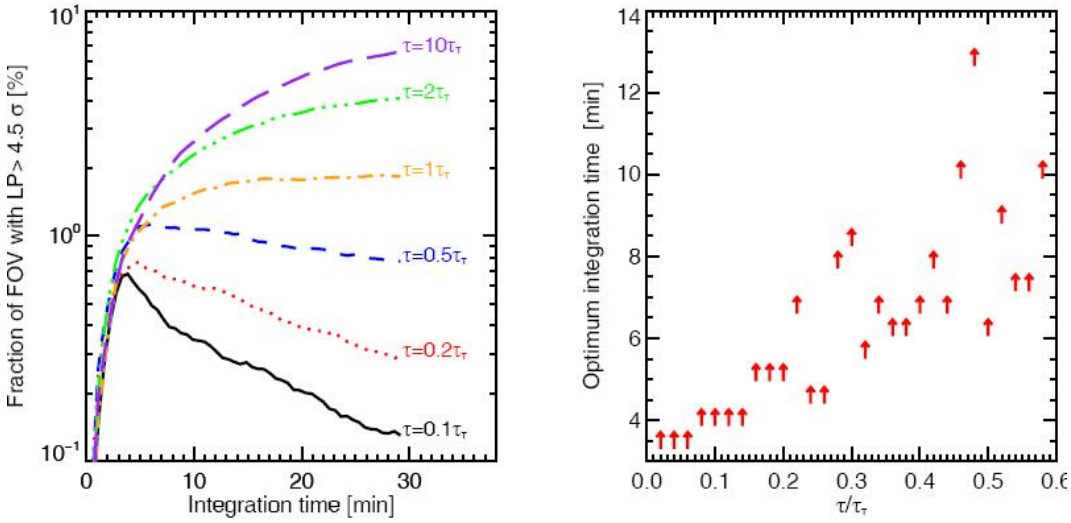

Figure 3: Area coverage of linear polarization signals larger than 4.5σ noise level versus integration time, for different distributions of lifetime of magnetic patches with different e-foldings (τ_T). All features are assumed to have the same size of 0.1 arcsec^2 and the same LP_{max} of 18.7×10^{-4} (left panel). Movement of peak position (i.e., the amount of optimum integration time which leads to the maximum area coverage of signals) with variable e-folding (τ_T=92 s) of lifetime distribution of patches (right panel).

amplitude) on the results, we simulated images for different distributions of these parameters (i.e., exponential distributions with different e-foldings). Thus the distribution of one of the three quantities is variable while the other parameters are left unchanged.

3.2.3 The effect of patch lifetime

To study the effect of lifetime of the magnetic patches on the optimum integration time of maps, we assume a variable e-folding (τ_T=92 s) ranging from $0.1\tau_T$ to $10\tau_T$ for the lifetime distributions. All patches are considered to have the same size of 0.1 arcsec^2 and same $LP_{max} = 18.7 \times 10^{-4}$.

Left panel of Figure 3 represents the fractional coverage of pixels with SNR$\geq$ 4.5 for different distributions of lifetime. For relatively short-lived patches, the graph mimics the behavior of the linear polarization component, from the IMaX data (appearance of a peak; Figure 2d). For these cases, it is also seen that position of the peak (the amount of optimum integration time which leads to a maximum area coverage of signals) shifts towards shorter integration times with smaller τ (right panel of Figure 3). Figure 3 (right) display dependence of peak position to the lifetime distribution of patches. For long-lived patches, it resembles the Figure 2c, i.e., the variation of significant signal coverage of CP with integration time.

3.2.4 The effect of patch size

Figure 4 (left panel) illustrates the effect of the size of the magnetic patches on the results. Variable e-foldings ($\tau_s = 0.24\ arcsec^2$) between $0.1\tau_s$ to $10\tau_s$ are considered for the size of magnetic patches while a constant lifetime of 100 s and a constant $LP_{max} = 18.7 \times 10^{-4}$ are

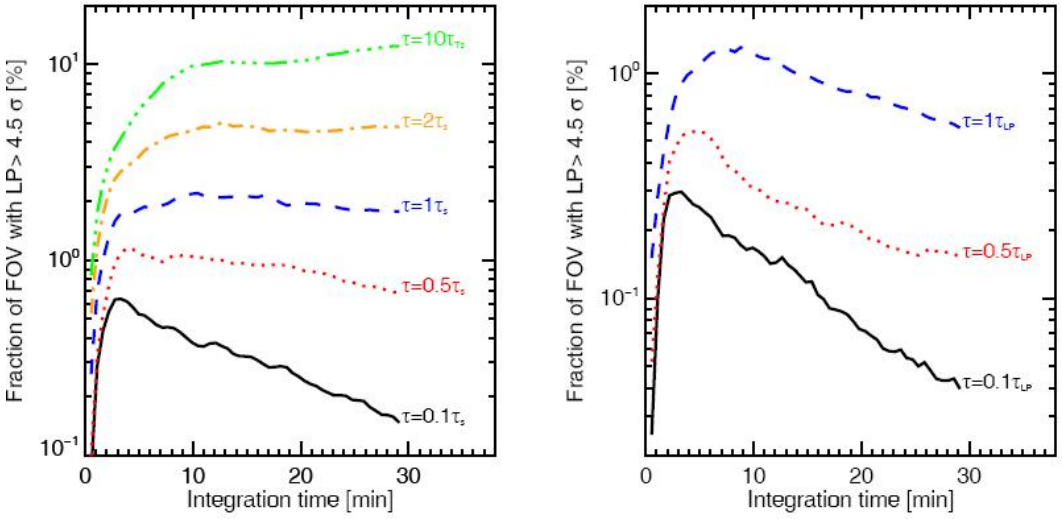

Figure 4: Same as Figure 3, but for different distribution of size of magnetic patches with different e-foldings of τ_S. Constant values for the lifetime and LP_{max} equal to 100 s and 18.7×10^{-4} are respectively assumed for all patches (left panel). Same as Figure 3, but for different distributions of LP_{max} of magnetic patches with different e-foldings of τ_{LP}. Both sizes and lifetimes of the patches are assumed unchanged equal to 100 s and 0.1 arcsec^2, respectively (right panel).

assumed. It is seen in Figure 4 (left panel) that curves get shallower on the left side of the peak for larger magnetic patches and drop slower, since larger patches more likely overlap each others. The larger the patches, the more monotonic the behavior of the variation of coverage of the FOV with detectable signal versus integration time are exhibited.

3.2.5 The effect of patch amplitude

In order to study the effect of different amplitudes of the magnetic patches, simulations for patches with constant size and lifetime of $0.1 arcsec^2$ and 100 s, respectively, but with variable e-foldings ($\tau_{LP} = 4.5 \times 10^{-4}$) ranging from $0.1\tau_{LP}$ to $10\tau_{LP}$, are performed (right panel of Figure 4).

From Figures 4, it is seen that finite lifetime of the patches, restricts the enough integration of the images to achieve the best SNR. Even for very large patches, integration seems to be effective till a finite time. Further integration leads to be seen an unchanged value or very slowly increasing behavior for the SNR.

Finally we provide a simulation for the case that all the three parameters (i.e., size, lifetime, and LP_{max}) differ for different patches (i.e., each has an exponential distribution with e-folding of τ_s, τ_T and τ_{LP} respectively.) and are coupled via equations 3 and 4 (see Figure 5).

4 Conclusions

Motivated by earlier work [19, 4], we have investigated a proper temporal-integration of the polarization signals with which an optimum SNR could be obtained. We used time-series

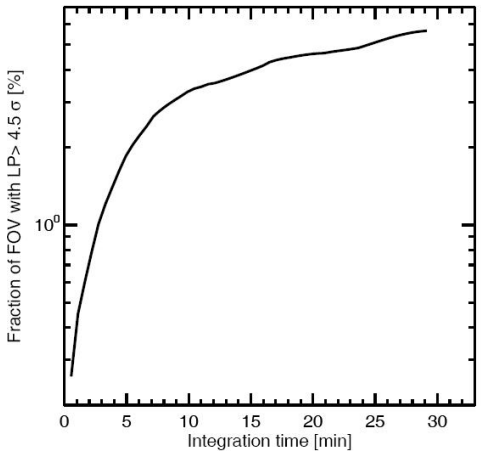

Figure 5: Fraction of the area covered by signals larger than 4.5σ noise level as a function of integration time, for synthesized polarization maps. Exponential with e-folding of τ_T, τ_S and τ_{LP} are assumed for distribution of lifetime, size, and amplitude of the patches. Each of these three parameters are coupled together via the Eqs. 3, 4.

.

of Stokes parameters from SUNRISE/IMaX to investigate the behavior of variation of SNR improvement with integration time.

We found that the fraction of area with a detectable linear polarization signal (i.e., when SNR$\geq$ 4.5) increases by increasing the temporal-integration time up to about 8 minutes (see Figure 2d). This variation is, however, different for the circular polarization signal. For CP, the fraction of FOV with SNR$\geq$ 4.5 shows a rapid increase up to 3 minutes integration, then it continues to increase with integration time up to about 8 minutes. After that, it basically saturates.

Danilovic et al. [9] have detected 4536 temporal magnetic features, appearing and disappearing in about 2000 arc second square in 30 minutes. The lifetime distribution of their linear magnetic features peaks at 100 s with an extended tail that can be fitted with exponential. From their Figure 2a, we estimated a mean lifetime of 92 s for the linearly polarized features. Visual inspection of the images of the linear and circular polarization shows that actually there are a few large and long life magnetic features which make the constant tail of the circular polarization plot in Figure 2, although the major contribution to those pixels with linear polarization above 4.5 σ coming from short-lived patches.

Statistically, a signal that is submerged in the noise can be extracted and detected after a long-enough temporal integration (as long as the signal exists). This is because that the signal amplification is proportional to integration time which is much faster than that of the noise which grows proportional to square root of integration time (for photon noise). For a static and long-lived (or permanent) magnetic patch, a very large SNR improvement can be achieved (i.e., with a long temporal integration comparable to the feature's lifetime). The SNR of a short-lived feature may, however, be improved up to a temporal integration whose length is given by the feature's lifetime. Further integration reduces the SNR again. (see Figure 2d).

We also explored the variations of coverage of detectable signals with integration time with the help of a simple numerical simulation. This clarified that the behavior of the variations strongly depended on lifetime and size of the magnetic features. As evidenced

in Figures 3 and 4, the curves do not show any peak (corresponding to an integration time with optimum SNR) when relatively long-lived or relatively large magnetic patches exist in the FOV. Therefore, the existence of relatively large and long-lived magnetic patches in the FOV, that are mostly corresponded to the network elements (for the linear polarizations) results in an apparent monotonic improvement of the amount of detectable signals that do not necessarily represent the improvement of all signals in the FOV. In particular, such an improvement does not correspond to the relatively small and short-lived linear magnetic patches in internetwork areas. The maximum temporal-integration time of $\approx$ 8 minutes determined from the SUNRISE/IMaX observations agrees with those from our numerical simulations .

The results of our simulations may explain Figure 2 of the paper by Bellot et al. [4], where coverage of the significant linear signals monotonically increase with integration time. This could be due to the presence of large and long-lived magnetic patches in the FOV of their observations (see Figure 4 of their paper). In addition, we found a similar monotonic curve for the CP from the same dataset as they used in their study (but with much steeper increase and much larger SNR improvement, compared to the one for the LP in Figure 2 of their paper). Therefore, only based on such monotonic increases of LP and CP with integration time, the same statement as for the LP (i.e. pervaded horizontal field in the IN) could be also valid, even stronger, for the CP variation.

Summarizing, we conclude that temporal integration of polarization signals can indeed improve the SNR. However, the maximum allowed integration time is strongly limited to the lifetime and size of the magnetic features and also to the dynamical time-scale of the solar granules on the solar surface. Longer integration times would misinterpret the data, since the apparent SNR improvement could be due to, e.g. few longer-lived magnetic patches in the FOV, and not to smaller features.

References

[1] Alissandrakis, C. E., Dialetis, D., Tsiropoula, G. 1987, A&A, 174, 275

[2] Asensio Ramos, A. 2009, ApJ, 701, 1032

[3] Barthol, P., Gandorfer, A., Solanki, S. K., et al. 2011, Sol. Phys., 268, 1

[4] Bellot Rubio, L. R. , Orozco Surez, D. 2012, ApJ, 757, 19

[5] Berkefeld, T., Schmidt, W., Soltau, D., et al. 2011, Sol. Phys., 268, 103

[6] Bommier, V., Martnez Gonzlez, M., Bianda, M., et al. 2009, A&A, 506, 1415

[7] Borrero, J. M. , Kobel, P. 2011, A&A, 527, A29

[8] Borrero, J. M. , Kobel, P. 2012, A&A, 547, A89

[9] Danilovic, S., Beeck, B., Pietarila, A., et al. 2010, ApJ, 723, L149

[10] Gandorfer, A., Grauf, B., Barthol, P., et al. 2011, Sol. Phys., 268, 35

[11] Giannattasio, F., Del Moro, D., Berrilli, F., et al. 2013, ApJ, 770, L36

[12] Hirzberger, J., , Feller, A., Riethmller, T. L., et al. 2010, ApJ, 723, L154

[13] Hirzberger, J., Bonet, J. A., Vzquez, M., Hanslmeier, A. 1999, ApJ, 515, 441

[14] Ishikawa, R. , Tsuneta, S. 2009, A&A, 495, 607

[15] Jafarzadeh, S., Cameron, R. H., Solanki, S. K., et al. 2014a, A&A, 563, A101

[16] Jafarzadeh, S., Solanki, S. K., Feller, A., et al. 2013, A&A, 549, A116

[17] Jafarzadeh, S., Solanki, S. K., Lagg, A., et al. 2014b, A&A, 569, A105

[18] Lamb, D. A., Howard, T. A., DeForest, C. E. 2014, ApJ, 788, 7L

[19] Lites, B. W., Kubo, M., Socas-Navarro, H., et al. 2008, ApJ, 672, 1237

[20] Lites, B. W., Leka, K. D., Skumanich, A., Martnez Pillet, V., Shimizu, T. 1996,ApJ, 460, 1019

[21] Lites, B. W., Socas-Navarro, H., Kubo, M., et al. 2007, PASJ, 59, 571

[22] Martnez Pillet, V., Del Toro Iniesta, J. C., lvarez-Herrero, A., et al. 2011, Sol. Phys., 268, 57

[23] Orozco Surez, D. Bellot Rubio, L. R. 2012, ApJ, 751

[24] Orozco Surez, D., Bellot Rubio, L. R., del Toro Iniesta, J. C., et al. 2007a, ApJ, 670, L61

[25] Orozco Surez, D., Bellot Rubio, L. R., del Toro Iniesta, J. C., et al. 2007b, PASJ, 59, 837

[26] Snchez Almeida, J. 2004, Astrophys. Space Phys. Res., 325, 115

[27] Solanki, S. K., Barthol, P., Danilovic, S., et al. 2010, ApJ, 723, L127

[28] Stenflo, J. O. 2010, A&A, 517, A37

[29] Title, A. M., Tarbell, T. D., Topka, K. P., et al. 1989, ApJ, 336, 475